Emission intermittency in silicon nanocrystals

Frank Cichos*
Photonics and Optical Materials, Institute of Physics, Chemnitz University of Technology, D-09107 Chemnitz, Germany

Jörg Martin† and Christian von Borczyskowski‡
Optical Spectroscopy and Molecular Physics, Institute of Physics, Chemnitz University of Technology, D-09107 Chemnitz, Germany
(Received 11 March 2004; revised manuscript received 17 June 2004; published 21 September 2004)

We present detailed results of blinking studies on individual silicon nanocrystals. The experiments show, that similar to II-VI semiconductor nanocrystals, the blinking process obeys a power law statistics. An excitation intensity dependence of the power law exponent is found for the *off* time probability distribution. The intensity dependence is interpreted in terms of an intensity dependent tunneling rate due to Auger assisted processes. Further we demonstrate a relation of the *off* time distribution to the bleaching and recovery of the emission of nanocrystal ensembles, which gives further insight in the blinking behavior according to ensemble studies. The experimental data is discussed in terms of two alternative blinking models. Evidence is provided for the existence of self-trapped polaron-like states for the ejected charge.

DOI: 10.1103/PhysRevB.70.115314 PACS number(s): 78.67.Bf, 73.22.Dj, 78.55.Ap, 78.67.Hc

I. INTRODUCTION

Semiconductor nanocrystals are of growing interest due to their tunable optical properties based on quantum confinement effects. They are discussed as fluorescent labels[1] or are applied in active optical structures.[2] One of the surprising properties of a single semiconductor nanocrystal is the emission intermittency or blinking which is similar to the well known effect for single molecules. However, the nature of this effect might be different, due to the different electronic structure, i.e., the density of electronic states. This emission intermittency is the subject of a number of recent studies, which reveal a rather complex behavior.[4] Most of these studies focus on the blinking observed in II-VI semiconductors such as CdSe, CdS, or CdTe.[5–8] Only a few studies demonstrate the feasibility of blinking studies on silicon nanocrystals.[9–13] However, it lacks a more detailed view on these particles since silicon is the most important semiconductor in microelectronics. Further, there is also a profound interest of astrophysics in these nanocrystals, since they are supposed to contribute to the so called "extended red emission"—an emission feature of interstellar dust which is currently not clearly assigned to a specific carrier.[15,16]

The main difference between the II-VI nanocrystals and silicon nanocrystals lies in the indirect band gap of silicon. This turns bulk silicon into a poor emitter. However, it has been shown, mainly along the discovery of porous silicon,[17] that silicon can efficiently emit light when the electronic excitation is confined in nanocrystals. Despite numerous studies, e.g., Refs. 9–11, 18, and 19 on silicon nanocrystals and porous silicon, a number of questions on the photophysics still remain open. Among them is the question of whether the different band structure compared with II-VI compounds causes any differences in the blinking behavior.

In this study we apply single particle spectroscopy and microscopy techniques to observe luminescence intermittency and to avoid the inhomogeneous spectral broadening of the emission. The addressing of individual particles allows us to observe the emission of just a single quantum object with a specific size. In order to discuss similarities and differences to II-VI semiconductor nanocrystals, we will discuss our results with respect to the recently published literature.[4,7,8,20,21]

II. EXPERIMENTAL

Silicon nanocrystal (SiNC) samples are prepared from porous silicon. *P*-type silicon (boron doped) is etched at a current density of $5-10\ \mathrm{mA/cm^2}$ for 180 minutes and transformed into porous silicon (ps). The emission spectrum of the final ps-sample ranges from 530 nm to 750 nm and peaks at 650 nm. After etching the sample is rinsed in ultrapure water and then sonicated in toluene. The solution is then diluted and spin casted onto a quartz substrate.

Blinking time traces, spectra and bleaching effects of larger ensembles are recorded in a home built confocal microscope. The light from an argon ion or krypton laser (514 nm or 482 nm) is coupled into the microscope by a glass wedge. The excitation light is focused onto the sample on top of a piezo scanner with a Zeiss 100x/0.9NA microscope objective. The emission is collected by the same objective and imaged onto an avalanche photodiode (EG&G) and onto a spectrograph coupled to a liquid nitrogen cooled CCD (Princeton Instruments). Emission time traces were recorded at two excitation power levels at $1.3\ \mu\mathrm{W}$ ($1.8\ \mathrm{kW/cm^2}$) and $4.6\ \mu\mathrm{W}$ ($6.5\ \mathrm{kW/cm^2}$), respectively.

III. RESULTS

To estimate the size of the particles, which are removed from the porous silicon by the sonification process, we recorded emission spectra of the porous silicon structure before and after the ultrasonic treatment under the same conditions. The difference spectrum is shown in Fig. 1(a). The spectrum peaks at 600 nm and has a half width of about 110 nm. From the comparison of this emission wavelength with theoretical

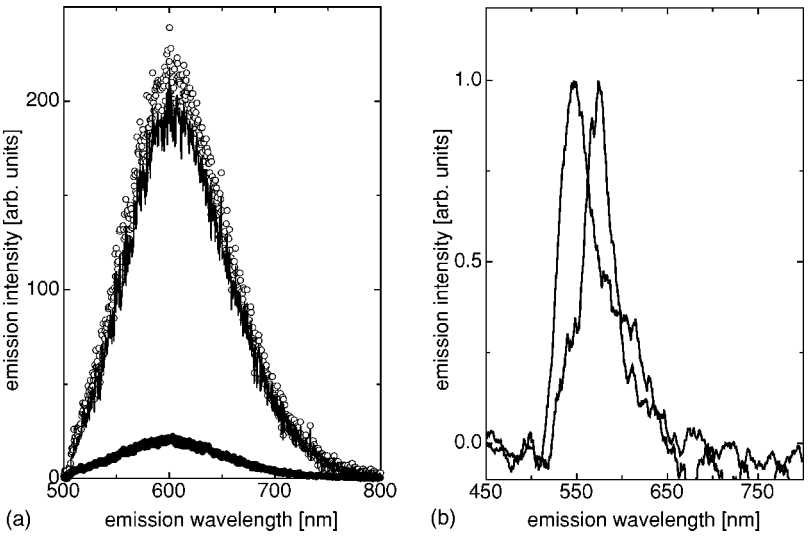

FIG. 1. (a) Difference emission spectrum of the porous silicon sample before and after the ultrasonic treatment (solid line) together with the emission spectra of porous silicon before (open circles) and after (closed circles) the ultrasonic treatment. (b) Emission spectra of two single silicon nanoparticles.

predictions of quantum confinement[22] we estimate a nanocrystal diameter of about 2.5 nm. Since no reliable high resolution electron microscopy data is available on the SiNC size distribution, we estimate the width of the size distribution by comparing the width of the emission spectrum to the data for size selected SiNC in Ref. 3. The measured spectral width of the difference spectrum of 110 nm thus corresponds to a FWHM of the size distribution smaller than 1 nm.

Figure 1(b) displays the emission spectra of two different particles. Obviously particles with a different center wavelength of emission can be found. As expected, the emission spectra are narrower than the difference spectrum. A FWHM of about 1200 cm^{-1} is found. Further, in some cases, the emission spectra seem to be structured with a side band at about 1000 cm^{-1} to the low energy side of the main peak. Since the emission of individual particles and the difference spectra taken from the porous structure nicely agree, we relate the observed emission to the emission of single SiNC. The assumption of single nanoparticles is strongly supported by the observation of emission intermittency.[10,23] However, the low emission rates and the statistics of the emission intermittency (short *on* times) make it extremely difficult to record emission spectra, with a sufficient signal to noise ratio. Therefore we are not able to provide enough spectra of single SiNC to resemble the difference spectrum.

To compare the blinking behavior of these silicon nanocrystals with II-VI semiconductor nanocrystals, we recorded emission time traces of individual particles. About 100 particles have been studied, each over the course of 1 minute with a bin time of 10 ms. All particles are photostable, which means that they emit at least up to 20 minutes. The emission time traces mainly consist of short *on* times (on the order of 100 ms) interrupted by long *off* times (several 100 ms) at all excitation intensities. To characterize the blinking behavior of the particles we calculate the statistics of *on* and *off* time durations for each emission time trace. Figures 2 and 3 contain the results for all measured particles. Both *on* and *off* time statistics show a nonexponentially decreasing probability for increasing *on* and *off* times. The probability distribution can be well fitted over a large range by a power law,

$$p(t_{on/off}) = p_0 t^{-\alpha_{on/off}}, \tag{1}$$

where p_0 is a constant to normalize the first bin to one. The *on* time distribution is best fitted with an exponent of $\alpha_{on} = 2.2(\pm 0.1)$ and is independent of the excitation power. The *off* time distribution bends from an exponent of about $\alpha_{off} = 1.3(\pm 0.05)$ for short *off* times to an exponent of about $\alpha_{off} = 1.7(\pm 0.1)$ for long *off* times at low excitation power. Further the *off* time distribution depends on the excitation power. At higher excitation power (4.6 μW), the bending behavior almost completely disappears and α_{off} becomes 1.3(±0.05). The insets of Fig. 2 and 3 show that the power law is not the result of the compilation of many particle data.

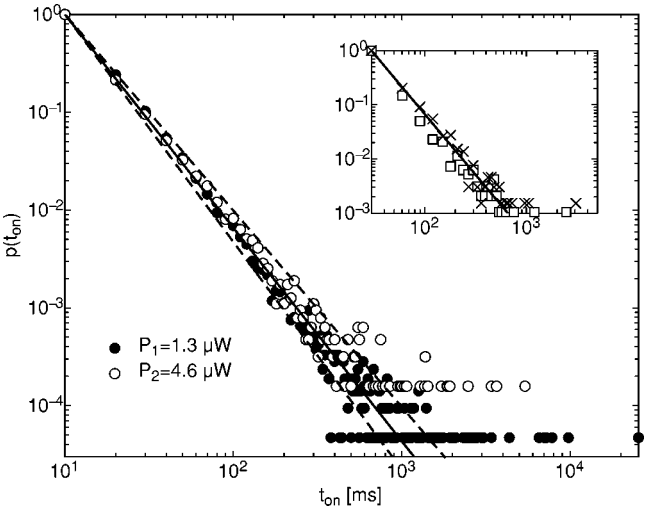

FIG. 2. *On* time statistics of silicon nanoparticles compiled from 100 individual emission time traces. The closed symbols correspond to an excitation power of 1.3 μW, the open symbols to an excitation power of 4.6 μW. The solid line is a fit to the data with a power law $p(t_{on}) = p_0 \cdot t^{-\alpha_{on}}$ with $\alpha_{on} = 2.2$. The dashed lines correspond to a power law with $\alpha_{on} = 2.1$ and $\alpha_{on} = 2.3$, respectively. The inset shows the *on* time statistics for two single silicon nanocrystals, which obey the same power law behavior as the ensemble.

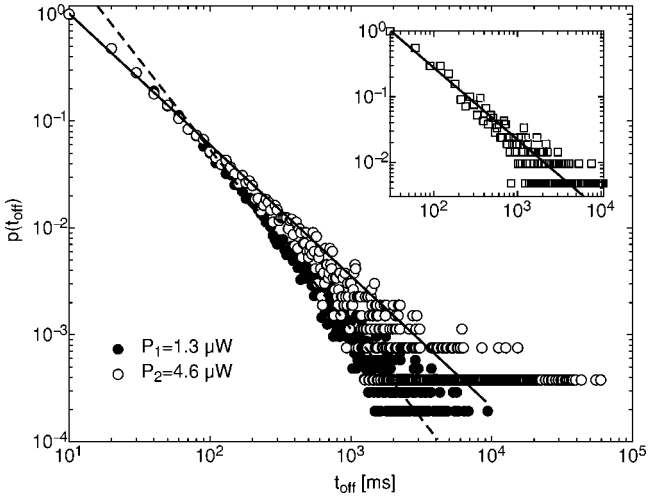

FIG. 3. *Off* time statistics of silicon nanoparticles compiled from 100 individual emission time traces. The closed symbols correspond to an excitation power of 1.3 μW, the open symbols to an excitation power of 4.6 μW. The solid line is a fit to the data with a power law $p(t_{off})=p_0 \cdot t^{-\alpha_{off}}$ with $\alpha_{off}=1.3$. The dashed line corresponds to a power law with $\alpha_{off}=1.7$. The inset shows the *on* time statistics of an individual silicon nanocrystal.

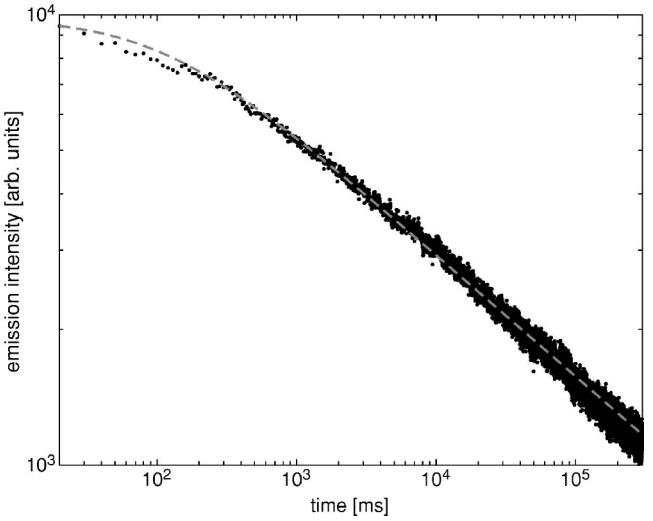

FIG. 4. Photobleaching of silicon nanocrystals in a porous silicon sample. The dashed line is a fit to the data with a power law $I(t) \propto (t+\tau_0)^{-\beta}$ with $\tau_0=111$ ms and $\beta=0.3$.

Individual particles, as far as they give enough events, clearly show the same power law statistics as the average of all measured particles.

One of the characteristics of the probability distribution as found for the *off* times is that the distribution has no finite mean. The integral

$$\langle \tau \rangle = \int_{t_0}^{\infty} tp(t)dt \tag{2}$$

diverges, in case $p(t)$ obeys a power law [Eq. (1)] with an exponent $\alpha<2$ (a lower boundary t_0 has to be defined, since the *off* time cannot become infinitely short which would turn the quantum efficiency to zero). This has important consequences on the stationarity of the blinking process.[24] The mean *off* time will thus tend to infinity and therefore depends on the observation time itself. The power law statistics of the *off* times with an infinite mean is therefore directly connected to a nonstationary behavior of the average *off* time. Therefore the emission intensity of an ensemble should decrease with increasing observation time, which leads to an apparent bleaching as described in Ref. 24 for CdSe nanocrystals. We indeed observe a bleaching effect for an ensemble of SiNC (porous silicon) as shown in Fig. 4. If this bleaching is based on the power law statistics of the blinking process, it has to be reversible. The reversibility is demonstrated by the following experiment: We first bleach the nanocrystal ensemble for 10 seconds. Then, the laser is switched *off* for a variable waiting time $\Delta\tau$ and switched on again after $\Delta\tau$. The intensity trace of the bleaching process consists therefore of two emitting periods as shown in Fig. 5(a). To measure the recovery from bleaching we calculate the ratio of the re-gained emission intensity in the second period compared to the bleached intensity from the first period as a function of the waiting time $\Delta\tau$. The result is shown in Fig. 5(b). The intensity ratio is increasing from about 0.35 at $\Delta\tau=10$ s to 0.7 at $\Delta\tau=300$ s. Clearly this observation deviates from a typical irreversible photochemical bleaching process.

IV. Discussion

A. Bleaching behavior

The bleaching (time dependent emission intensity) curve in Fig. 4 should represent the fraction of particles which are in the *on* state at a certain time. In the model described in Ref. 24 this fraction is simply proportional to $t^{\alpha_{off}-\alpha_{on}}$, since both *on* and *off* time distributions follow a power law with an exponent $\alpha<2$. However, in our case the *on* time distribution has a finite mean and the bleaching behavior is not described by the former relation. We have applied Monte Carlo simulations to obtain a numerical form of the bleaching curve. We simulate emission time traces of single nanocrystals by taking random samples out of a power law distribution constructed by the model described in Ref. 7 to obtain *off* times. The power law exponent has been adjusted to 1.9, 1.5 and 1.3 to obtain the relative photoluminescence intensities depicted in Fig. 6. The *on* times are assumed to be of constant length (*on* time distribution has a finite mean value). A sequence of *on* and *off* times then resembles an emission time trace with 1 representing the *on* state and 0 for the *off* state. Each emission time trace is simulated until the sum of *on* and *off* times reaches a length of 5×10^3 (arbitrary units). At this time we start the simulation of the recovery of emission until a total length of each time trace of 10^4 (arbitrary units) is reached. To obtain the intensity recovery nanocrystals are assumed not to enter the *off* state anymore beyond $t=5\times10^3$. The nanocrystals return from their *off* state at a certain time if they were *off* at $t=5\times10^3$ or stay in the *on* state if they were *on* at $t=5\times10^3$. To obtain the bleaching and recovery curves we simulated a total number of 10^4 time traces. The bleaching and recovery is quantified by counting

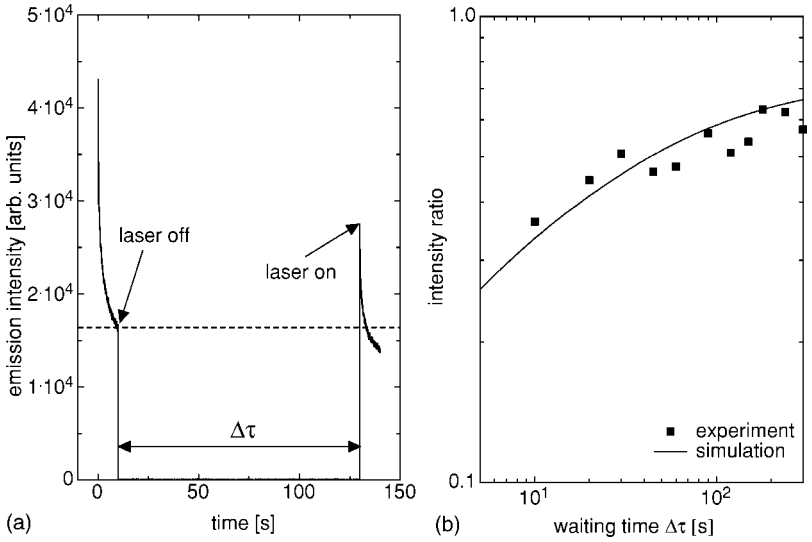

FIG. 5. (a) The graph shows the emission intensity of a silicon nanocrystal of porous silicon as a function of time (bleaching). After 10 s the excitation laser is switched off and switched on after a variable time $\Delta\tau$. (b) Ratio of the recovered intensity after time $\Delta\tau$ and the initially bleached intensity as a function of the waiting time $\Delta\tau$ together with a recovery curve from a Monte Carlo simulation for a power law *off* time statistics with $\alpha_{off}=1.7$ (see the text for details).

the number of traces which are in the *on* state in the interval $[t,t+\Delta t]$ with $\Delta t=1$. This number corresponds then to the ensemble intensity at a time t in the experiment. We find that all results of simulated bleaching curves can be well fitted with a power law according to $I=I_0(t+\tau_0)^{-\beta}$, where τ_0 is related to the mean *on* time (ensuring a finite intensity at $t=0$). The exponent β is empirically found to follow $\beta=2-\alpha_{off}$, where α_{off} is the exponent of the *off* time statistics. As shown in Fig. 4 this power law fits the experimental data well with the parameters $\tau_0=111$ ms and $\beta=0.3$. The value found for β corresponds to an exponent $\alpha_{off}=1.7$ for the *off* time distribution as compared to $\alpha_{off}=1.7$ found experimentally for a long *off* time at 1.3 μW excitation power. Indeed this relation between β and α_{off} is reasonable since the way the emission intensity is decaying is related to growth of the mean *off* time to infinity. This growth is given by

$$\langle\tau(t_u)\rangle = \int_{t_0}^{t_u} tp(t)dt = \int_{t_0}^{t_u} tt^{-\alpha_{off}}dt \propto \frac{-t_u^{2-\alpha_{off}}}{\alpha_{off}-2}, \qquad (3)$$

with $p(t)$ being the *off* time probability distribution. The growth of $\langle\tau(t_u)\rangle$ is determined by a power law with an exponent which indeed resembles the relation between β and α_{off} found in the simulations and shows that the bleaching has to disappear for $\alpha_{off}>2$, when a finite mean *off* time can be defined. Further, a slowly decaying power law distribution for the *off* times (α_{off} considerably smaller than 2) causes an increasing mean *off* time which drives the ensemble into a state with low emission intensity. Therefore the bleaching has to be faster for α_{off} values considerably smaller than two. In a similar way the recovery can be explained qualitatively. The recovery is related to the return from the *off* state, which is expressed by the *off* time distribution. An *off* time distribution with a large α_{off} will therefore result in a fast recovery. A summary of this behavior found from Monte Carlo simulations is depicted in Fig. 6, which shows the bleaching and recovery of an ensemble of nanoparticles for different α_{off}. In addition, a Monte Carlo simulation of the recovery for an *off* time distribution with $\alpha_{off}=1.7$ is displayed in Fig. 5(b) in comparison with the experimental data, which demonstrates again the relation of blinking, bleaching and emis-

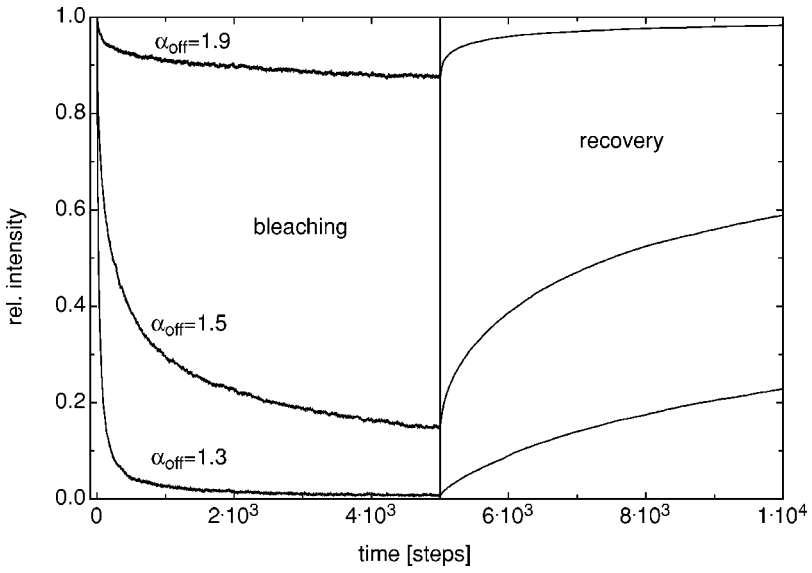

FIG. 6. Simulated bleaching and recovery curves for an ensemble of nanocrystals with different power law distributions for the *off* times (*on* times of constant length). The curves show the relative intensity $I(t)/I(t=0)$. The power law distributions for the *off* times are generated with the model of Verberk *et al.* (Ref. 7). After 5×10^3 timesteps, the system is not allowed to enter the *off* state after the previous *on* time. The ensemble intensity thus only depends on the number of particles that have returned from the last *off* event.

sion recovery. We are therefore qualitatively and quantitatively able to predict the bleaching and emission recovery of nanocrystal ensembles from the blinking statistics of single crystals and *vice versa*. This gives an additional tool to study the nanocrystal blinking behavior especially at long times, where it is commonly difficult to obtain good statistics from single nanocrystal emission time traces.

B. Ionization pathways

The observed blinking behavior directly shows the existence of a dark state, which is commonly assumed to be a charged state[7,8] where the electron of the excited electron hole pair is ejected to trap states in the vicinity of the nanocrystal. The free carrier in the nanocrystal core can efficiently quench further optical excitations by an Auger process until the particle is neutralized by the return of the electron.[25] The Auger process causes a very fast and nonradiative depopulation of the excited state. If the Auger process is much faster than the radiative lifetime, the Auger process will dominate and the particle will be essentially dark. The radiative lifetime of SiNC is on the order of a few microseconds corresponding to a rate of 10^5 to 10^6 s^{-1}, while the reported values for the energy transfer to the free carrier are around 200 ps.[26] Thus quenching via an Auger process is highly efficient and we assume that this mechanism is responsible for the observed dark state of SiNC. A further requirement for this dark state is the ejection of a charge out of the SiNC core. Indeed a number of experiments on single CdSe nanocrystals provide evidence for a nanocrystal ionization in the dark state.[6,14] Among them is the observation of spectral diffusion, which is explained in terms of an exciton interaction with localized charges. While measurements of spectral diffusion on SiNC are in principle possible, the extremely low amplitude for long *on* periods in the emission time traces $[p(t_{on}=1\ \mathrm{s}) \approx 4\times 10^{-5}]$ and the low emission rates prevent an efficient recording of emission spectra with a reasonable time resolution. However the SiNC charging and the related optical ensemble properties are discussed in several other references (see Ref. 18).

Possible mechanisms for the ejection of a charge from the SiNC are illustrated in the energy level scheme in Fig. 7. The energy level scheme has been constructed from the band offset between the conduction band of bulk silicon and the conduction band of silicon dioxide which has been reported to be about 3.5 eV.[27] We have then shifted the valence and conduction band of silicon to typical gap values of SiNC which are around 2.1 eV. The conduction band and the valence band have been shifted according to the effective mass approximation with a ratio of effective masses of electron and hole of 0.19/0.49.[28] The level scheme provides an idealized picture of the SiNC core, since it relies on the bulk silicon dioxide band gap even though this value is likely to depend on the thickness of the silicon dioxide layer. However, the scheme should give an idea about the possible ionization mechanisms. As shown in Fig. 7 the band offset between the SiNC core and the silicon dioxide shell is about 2.7 eV, which rules out a thermal ejection of an electron directly from the conduction band. A possible thermal ejection may however still occur via an Auger assisted process. In such an Auger assisted process two excitons are created by subsequent optical excitations. One of the excitons recombines by releasing its energy to the second exciton. This leads to a maximum excitation of the residual exciton by the emission energy (about 2.1 eV) resulting in the state AA (see Fig. 7). The Auger assisted process therefore diminishes the barrier to $\Delta E_{AA}=0.6$ eV and increases the probability of thermally assisted ionization. Estimating the rate of this Auger assisted thermal process according to an Arrhenius equation,

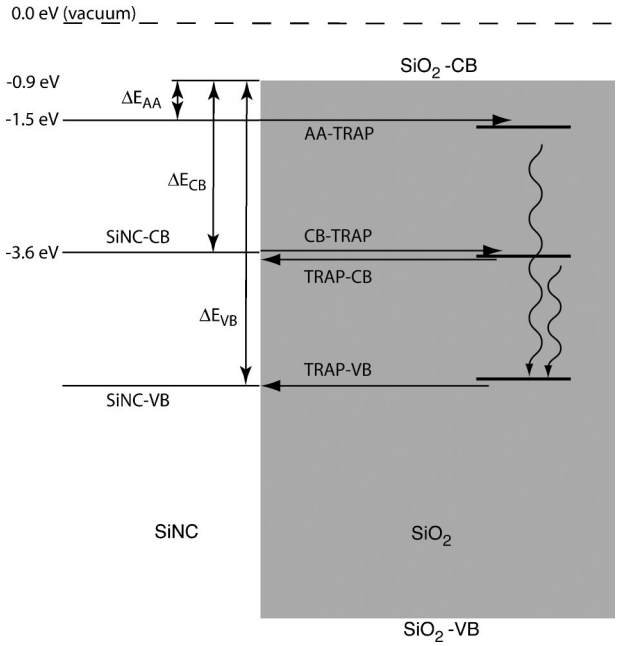

FIG. 7. Sketch of the electronic levels of the silicon nanocrystal including silicon dioxide conduction and valence band levels representative for the shell. The tunneling channels from and to the trap states are listed in Table I and marked with CB (conduction band), AA (Auger assisted) and VB (valence band).

$$k_{thermal} = Ae^{-\Delta E/k_B T}, \tag{4}$$

with a typical value of $A=10^{14}$ s^{-1} (eigenfrequency of the emitting exciton) and $\Delta E_{AA}=0.6$ eV leads to $k_{thermal} \approx 10^4$ s^{-1} at room temperature. Thus the Auger assisted thermal emission results in an ionization rate lower than the inverse radiative lifetime of the nanocrystal of 10^5 to 10^6 s^{-1}. Since two excitons have to be excited before this channel becomes active, this process will depend on the excitation intensity as well as on the temperature. Further, the above estimate assumes that the relaxation of the electron from the Auger excited state is much slower than the ionization rate. A fast dissipation of energy from the Auger excited to the lowest excitonic state will cause an additional decrease of the ionization rate. Therefore the value given above for the Auger assisted thermal ionization rate can be regarded as an upper limit. However, due to the low ionization rate in comparison with the emissive rate, this process should be of minor importance for the ionization.

A nonthermal ejection of charges is possible by a tunneling process from the nanocrystal to a trap state. A general

definition of the tunneling rate k_{tunnel} is given by the Bardeen formalism[29]

$$k_{tunnel} = \frac{2\pi}{\hbar} \int |M|^2 \rho_{NC}(E) \rho_{trap}(E) dE, \tag{5}$$

where M denotes the overlap matrix element of the exciton wavefunction and the trap wavefunction. ρ_{NC} and ρ_{trap} are the density of states of the nanocrystal and trap, respectively, and are a function of the energy E. Therefore the tunneling rate is influenced by all these parameters. A first approximation of the SiNC electronic density of states is given by a Delta function at E_{CB} and E_{VB}, since the quantum dot can be treated as a zero dimensional quantum confined system. Therefore elastic (resonant) tunneling can only occur if an unoccupied trap state exists at E_{CB}. Since we do not know the detailed nature of these trap states, we assume that the density of states of the trap is nonzero at E_{CB}. If we further assume a rectangular barrier and plane waves for the nanocrystal and the trap states, then the tunneling rate for an elastic tunneling process can be approximated by

$$k_{tunnel} = k_0 \cdot \exp\left(- \frac{2}{\hbar} \sqrt{2 m_e^* \Delta E} r \right), \tag{6}$$

where k_0 is the electron ringing rate, m_e^* is the tunneling effective electron mass [about $0.4 m_e$ (Ref. 30)], ΔE is the tunneling barrier and r is the tunneling distance. Again several tunneling pathways are possible. First, the electron may tunnel directly from the conduction band to a trap state. Thus according to Fig. 7, the tunneling barrier corresponds to $\Delta E_{CB} = 2.7$ eV. A tunneling distance of 1 nm and a ringing rate k_0 close to A (see thermal emission above) will lead to a tunneling rate of k_{tunnel} $(r = 1\ \text{nm}) = 5 \cdot 10^6\ \text{s}^{-1}$ which drops to k_{tunnel} $(r = 2\ \text{nm}) = 2.5 \times 10^{-1}\ \text{s}^{-1}$ for a distance of 2 nm. At a distance of 1 nm the tunneling rate therefore becomes comparable to the emission rate and thus influences the quantum yield of emission. If the excitation intensity is high enough an Auger assisted tunneling may occur. The tunneling barrier will then be $\Delta E_{AA} = 0.6$ eV which increases the tunneling rate to $3.7 \times 10^9\ \text{s}^{-1}$ for traps at 1 nm distance and $1.4 \times 10^7\ \text{s}^{-1}$ at a 2 nm distance, respectively. Therefore even at distances of 2 nm the Auger assisted tunneling to a trap will be faster than the lifetime of the SiNC and will thus effectively quench the emission. However, as noted above, these Auger assisted rates are upper limits of the tunneling rates, since our estimates do not include fast energy dissipation from the Auger assisted state to the CB. Therefore depending on this relaxation time, the tunneling rates will be between the values given for the tunneling from the CB and those for the Auger excited state. A rough estimation of the fraction of Auger excited electrons resulting in an ionized particle via tunneling from the Auger excited state gives about 4×10^{-3} assuming Auger assisted tunneling rates of about $3.7 \times 10^9\ \text{s}^{-1}$ and electron relaxation rates of about $1 \times 10^{12}\ \text{s}^{-1}$.

In summary the simple calculations above show, that if trap states with appropriate energies and at distances up to a few nm exist in the vicinity of the nanocrystal, tunneling processes provide a very efficient way to ionize SiNC.

C. Blinking statistics

1. Off time statistics

In the literature,[7,8] the power law statistic for the *off* times is explained in two different ways. Both models are based on a homogeneous distribution of trap states in the vicinity of the nanocrystal and can be understood as two special cases of a general model. The general model assumes a charge transfer from the nanocrystal to a trap state in the vicinity of the nanocrystal. The trap states are distributed homogeneously around the nanocrystal. The population and depopulation of traps occurs via charge tunneling (see Sec. IV B) from the nanocrystal (conduction band or Auger excited states) to a trap or from a trap to the nanocrystal (conduction or valence band). Further a charge exchange between the trap states is possible. The rate of exchange between trap states defines now the two special cases mentioned in the literature.

For the first special case we assume that the tunneling rate between different traps is high compared to the rate of direct return from the trap to the nanocrystal. The charges can then randomly walk through the trap state distribution and even escape to infinity. The return to the nanocrystal is then for long times determined by the random path the charge takes to return. This corresponds to a first passage problem of a random walker. The first passage time distribution will follow a power law,[31]

$$p(t) \propto t^{-3/2}, \tag{7}$$

with an exponent $\alpha = 1.5$ for long times t. This corresponds to the model proposed by Shimizu *et al.*[8] and which has also been discussed by Jung *et al.*[32] Indeed the assumption of an exchange between trap states seems to be reasonable, since if they are statically and homogeneously distributed over the matrix around the nanocrystal, they should have the same distance among each other as to the nanocrystal, which will result in an overlap of their wavefunction. Even though this picture is simplified and a more detailed, e.g., a biased random walk due to electron-hole Coulomb interaction should be considered, the random walk model gives a very intuitive way to explain power law statistics and other observations such as the described apparent bleaching (which also depends on the power law statistics). However, current observations including ours lead to exponents which differ from $\alpha = 1.5$ and therefore require a modification or refinement of this model, even including transport in fractal dimensions.

If we assume for the second special case of the general model no exchange (or very slow exchange compared to the direct tunneling from the nanocrystal to the core), then this model corresponds to the one by Verberk *et al.*[7] In this model, the charge will tunnel from the nanocrystal to a trap and back, without visiting a larger distribution of traps during an *off* period. The time for a charge to return is therefore directly related to the backward tunneling rate from the trap to the nanocrystal. Then the exponential distance dependence of the tunneling rate from the nanocrystal to the trap and back Eq. (6) leads to a power law statistics with a variable exponent. Verberk *et al.* have shown, that the exponent α_{off} has to be between 1 and 2. According to this model the exponent is defined by

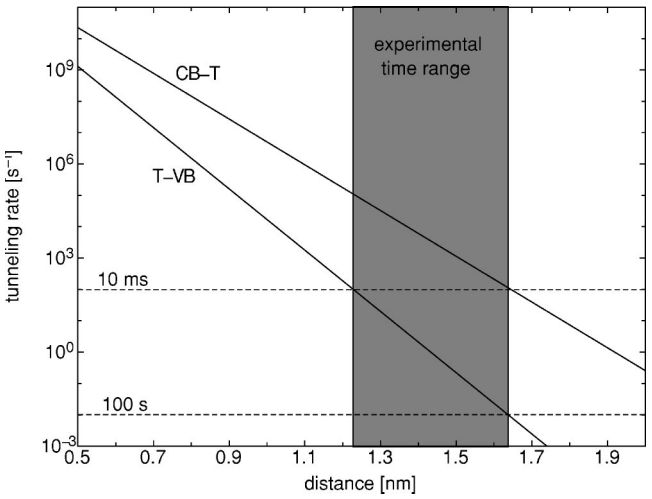

FIG. 8. Calculated tunneling rates corresponding to the energy level scheme provided in Fig. 7 according to Eq. (6). The shortcuts T-VB and CB-T denote a tunneling from the trap to the valence band and from the conduction band to the trap, respectively. We have marked the experimentally accessible range of time constants, which is from 10 ms to 100 s.

$$\alpha_{off} = 1 + \sqrt{\frac{\Delta E^{NC-T}}{\Delta E^{T-NC}}}, \tag{8}$$

where ΔE^{NC-T} is the barrier for tunneling from the nanocrystal to a trap and ΔE^{T-NC} the one for tunneling from a trap back to the nanocrystal. This model allows indeed for different exponents depending on the ratio of the tunneling barriers. However, since in this model the traps are assumed to be energetically degenerate, there must be some mechanism which prevents a fast exchange between traps but ensures the exchange between the nanocrystal and the trap. We will refer to a possible mechanism in Sec. IV D, where we will discuss the nature of the trap states.

It is currently not clear whether one of the special cases of this general model or a completely different model is appropriate to explain the experimental observations. However, since our experimental data show power law exponents between $\alpha_{off}=1.3$ and $\alpha_{off}=1.7$ for the *off* time statistics (error about ± 0.1), we assume a weak or even no exchange (random walk among traps) to be more realistic. This is further supported by the observed intensity dependence of the *off* time statistics. The random walk type model does not allow for intensity dependent *off* time statistics, since the type of ionization or the individual step for the exchange between traps is to a large extent irrelevant for the final statistics. However, such intensity dependent processes are possible in the second special case since the following ionization tunneling pathways exist (see Fig. 7): (1) tunneling of an electron directly from the conduction band to a trap state and (2) Auger assisted tunneling from $E_{CB}+2.1$ eV. This results in tunneling barriers of $\Delta E_{CB}^{NC-T}=2.7$ eV and $\Delta E_{AA}^{NC-T}=0.6$ eV, respectively. An elastic tunneling from the trap to the nanocrystal should occur at an energy level, where an accepting density of states exists in the core of the nanocrystal. Since the density of states in the energy gap of the nanocrystal is zero, we have to assume that a tunneling from the trap to the nanocrystal can only occur at the energy of the conduction band or the valence band. This results in the backward tunneling barriers $\Delta E_{CB}^{T-NC}=2.7$ eV and $\Delta E_{VB}^{T-NC}=4.8$ eV, respectively. The power law exponents for the *off* time statistics which are expected from the tunneling model [Eq. (8)] are summarized in Table I. The results show that a direct tunneling model (from a nanocrystal to a trap and back) with different tunneling pathways can indeed lead to power law exponents which are close to the experimentally observed ones. Further, an absorption cross section of 7×10^{-18} cm^2 (Ref. 18) (excitation 514 nm, emission detection at 576 nm) and excitation powers of 1.3 μW and 4.6 μW will lead to an excitation rate of about 3.26×10^4 s^{-1} and 1.17×10^5 s^{-1}, respectively. The average number of excitons in the nanocrystal is then given by the ratio of the excitation and emission rate, which is 0.32 for 1.3 μW and 1.2 for 4.6 μW. Assuming a Poisson statistics for the excitation light, the average population of 0.32 excitons corresponds to 86% single excitations and 14% double and higher excitations, while an average population of 1.2 corresponds to 52% single excitations and 48% double and higher excitations. The excitation of a second exciton is thus rather likely at an excitation power of 4.6 μW and the Auger assisted processes should become relevant in our experiments. Since the Auger assisted process is linked to changes in the tunneling barrier the power law exponent will depend on the excitation power too. According to the above considerations the exponent of the *off* time statistics should decrease from $\alpha_{off}=1.7$ to $\alpha_{off}=1.3$ with increasing excitation power. Indeed we observe this trend, since the excitation rate is just close to the emission rate. While at low excitation power an exponent of about $\alpha_{off}=1.7$ at the tail of the *off* time distribution is observed, this tail vanishes almost completely at higher excitation power, where we observe a power law with $\alpha_{off}=1.3$.

TABLE I. Possible pathways of tunneling from the SiNC core to trap states in the vicinity of the nanocrystal and related power law exponents for the off time statistics. The first column denotes the pathway (CB-conduction band, VB-valence band, AA-Auger assisted). The second and third column corresponds to the expected tunneling barriers according to the energy level scheme in Fig. 7. The fourth column gives the power law exponent according to Eq. (8) of the tunneling model of Verberk *et al.*

Pathway	Forward barrier (eV)	Backward barrier (eV)	Exponent α_{off}
CB-TRAP-VB	2.7	4.8	1.7
AA-TRAP-VB	0.6	4.8	1.3
AA-TRAP-CB	0.6	2.7	1.5

Even though the intensity dependence and the power law exponents fit to the described model, the *off* time statistics shows a kink where the exponent changes from about $\alpha_{off}=1.3$ to $\alpha_{off}=1.7$. Apparently short *off* times are connected to Auger assisted tunneling, while long *off* times are related to tunneling from the nanocrystals conduction band. This is at first glance contrary to expectation since a power law with $\alpha_{off}=1.3$ decays slower than the one with $\alpha_{off}=1.7$. The long

off times should thus be determined by the lower exponent. However, as mentioned at the beginning of the paper, the power law statistics is linked to a nonstationary photophysics, which causes, as shown in Figs. 4 and 5, the reversible bleaching of the ensemble and which is equivalent with a time dependent average *off* time. As noted at the end of Sec. III, this bleaching is faster for lower exponents of the *off* time statistics (bleaching with $t^{-2+\alpha_{off}}$). At long times, the ensemble bleaching is therefore determined by $\alpha_{off}=1.7$. Since the *off* time statistics is compiled from many particles, we suggest that this effect is responsible for the kink in the *off* time statistics.

2. On time statistics

So far we have discussed the *off* time statistics which is largely related to trap states, which are presumably located in the direct nanocrystal environment. The *on* times on the other hand are more closely connected to intrinsic properties of the nanocrystal. The number of channels which lead from the nanocrystal to a trap state and the characteristic times connected with these channels determine whether a simple exponential behavior (one channel) or a more complicated signature will be observed in the *on* time statistics. As in our case the *on* time statistics commonly also follows a power law statistics[7,8,21] even for a single particle. Since such power law statistics is related to a strong heterogeneity, the nanocrystal has to access a large variety of channels to the trap states. Due to the limited size of the nanocrystal the manifold of channels which are, i.e. caused by structural defects, are also limited and can thus not cause the observed power law statistics. Again, this difficulty can be tackled by the above described models. For instance Verberk *et al.* describe the power law observed for the *on* time statistics by allowing a charged nanocrystal to emit when the hole inside the ionized nanocrystal is not free but located at the CdSe/ZnS interface. Therefore *on* and *off* time statistics are directly linked to each other and should result in the same power law exponents. Obviously this model does not apply here. First of all, the *on* time exponent is with $\alpha_{on}=2.2$ quite different from the *off* time exponent. It even implies a finite mean *on* time, which is contrary to current findings for CdSe nanocrystals.[7,8,21] Further the model in Ref. 7 results in power law exponents which are limited to a range between one and two and the observed exponent is well outside this range. In a similar way there are no arguments which support a random walk type model for the *on* times; thus the power law statistics for the *on* times of SiNC remains the subject of further studies.

D. Nature of the trap states

One of the most puzzling phenomena of semiconductor nanocrystal emission intermittency is still the nature of the trap states. Even though we cannot provide more direct details about the trap states, the described model of the blinking allows an estimation of the trap density. This density of traps has to be rather high since as noted above only short distances (see Fig. 8) between the nanocrystal and the trap allow for an efficient exchange of charges between the nanocrystal and the trap. Moreover, only a sufficiently high number of trap states in the nanocrystal environment will lead to a power law distribution. Corresponding to the diffusion model the distance between two traps should be on the order of the distance between nanocrystal and trap. This distance is on the scale of a few nanometers, otherwise tunneling to the trap becomes inefficient. Similar conclusions can be drawn from the model of Verberk.[7] The tunneling rates from the CB to the trap and from the trap to the VB are shown in Fig. 8 as a function of the barrier width. Since in the model of Verberk the *off* times are determined by the tunneling rate from the trap to the nanocrystal, the traps have to be located at a distance of about 1.2 nm to 1.6 nm for typical timescales of our experiment. Again the distance between traps should therefore be on the nanometer scale or smaller. Both models require therefore a trap density, which is on the order of 10^{27} m^{-3}, which is certainly much too high for impurities or defect related states (silicon atomic density is about 5×10^{28} m^{-3}). Therefore we suppose the matrix itself provides the distribution of traps. Charges could be self-trapped via local polarization effects similar to polaron states. Such states are formed when the charge is ejected into the surrounding of the nanocrystal. An exchange between traps would then be equivalent to a hopping between self-trapped states, which should be very slow, due to the low electric conductivity of common polymer matrices or silicon dioxide. A slow hopping process would then favor the direct return of the charge to the nanocrystal and the system is in this case well described by the model of Verberk *et al.* The self-trapping nature of the states would possibly also allow us to explain the power law of the *on* time statistics. However, a more detailed spectroscopic analysis of such self-trapped states is necessary to explain the experimentally observed features.

V. CONCLUSIONS

In summary our studies show that the photophysics of SiNC is of similar complexity as for II-VI semiconductor nanocrystals. SiNC show an emission intermittency, which is goverened by power law statistics for the *on* and the *off* times. The *off* time statistics is intensity dependent and reveals several photoinduced ionization processes, which are interpreted in terms of Auger assisted and non-Auger assisted tunneling processes. The *on* time statistics is decoupled from the *off* time statistics, shows finite mean *on* time values and cannot be explained by current models which have been proposed for CdSe. The discussion of current models for the power law statistics leads to the conclusion that trap states are possibly related to self-trapped polaron-like states. Further, we have demonstrated that blinking, bleaching and emission recovery of SiNC are directly related to each other and may give valuable information on the long time behavior of the *on* and *off* time distributions.

ACKNOWLEDGMENT

This work has been supported by the DFG Research group 388 "Laboratory Astrophysics."

*Electronic address: cichos@physik.tu-chemnitz.de
†Electronic address: j.martin@physik.tu-chemnitz.de
‡Electronic address: borczyskowski@physik.tu-chemnitz.de

[1] J. M. Bruchez, M. Maronne, P. Gin, S. Weiss, and A. P. Alivisatos, Science **281**, 2013 (1998).
[2] H.-J. Eisler, V. C. Sundar, M. G. Bawendi, M. Walsh, H. I. Smith, and V. Klimov, Appl. Phys. Lett. **80**, 4614 (2002).
[3] G. Ledoux, O. Guillois, D. Porterat, C. Reynaud, F. Huisken, B. Kohn, and V. Paillard, Phys. Rev. B **62**, 15 942 (2000).
[4] M. Kuno, D. Fromm, H. F. Hamann, A. Gallagher, and D. J. Nesbitt, J. Chem. Phys. **112**, 3117 (2000).
[5] M. Nirmal, B. O. Dabbousi, M. G. Bawendi, J. J. Macklin, J. K. Trautman, T. D. Harris, and L. E. Brus, Nature (London) **383**, 802 (1996).
[6] R. G. Neuhauser, K. T. Shimizu, W. K. Woo, S. A. Empedocles, and M. G. Bawendi, Phys. Rev. Lett. **85**, 3301 (2000).
[7] R. Verberk, A. M. van Oijen, and M. Orrit, Phys. Rev. B **66**, 233202 (2002).
[8] K. T. Shimizu, R. G. Neuhauser, C. A. Leatherdale, S. A. Empedocles, W. K. Woo, and M. G. Bawendi, Phys. Rev. B **63**, 205316 (2001).
[9] M. D. Mason, G. M. Credo, K. D. Weston, and S. K. Buratto, Phys. Rev. Lett. **80**, 5405 (1998).
[10] F. Cichos, J. Martin, and C. von Borczyskowski, J. Lumin. **107**, 160 (2004).
[11] J. Valenta, R. Juhasz, and J. Linnros, Appl. Phys. Lett. **80**, 1070 (2002).
[12] J. Valenta, J. Linnros, R. Juhasz, F. Cichos, and J. Martin, in *Towards the First Silicon Laser*, edited by L. P. *et al.* (Kluwer Academic, New York, 2003), pp. 89–108.
[13] D. S. English, E. L. Pell, Z. Yu, P. F. Barbara, and B. A. Korgel, Nano Lett. **2**, 681 (2002).
[14] T. D. Krauss and L. E. Brus, Phys. Rev. Lett. **83**, 4840 (1999).
[15] G. Ledoux, O. Guillois, F. Huisken, B. Kohn, D. Porterat, and C. Reynaud, Astron. Astrophys. **377**, 707 (2001).
[16] A. N. Witt, K. D. Gordon, and D. G. Furton, Astrophys. J. **501**, L111 (1998).
[17] L. T. Canham, Appl. Phys. Lett. **57**, 1046 (1990).
[18] D. Kovalev, H. Heckler, G. Polisski, and F. Koch, Phys. Status Solidi B **215**, 871 (1999).
[19] G. Ledoux, J. Gong, F. Huisken, O. Guillois, and C. Reynaud, Appl. Phys. Lett. **80**, 4834 (2002).
[20] A. P. Alivisatos, J. Phys. Chem. **100**, 13226 (1996).
[21] M. Kuno, D. P. Fromm, S. T. Johnson, A. Gallagher, and D. J. Nesbitt, Phys. Rev. B **67**, 125304 (2003).
[22] M. V. Wolkin, J. Jorne, P. Fauchet, G. Allan, and C. Delerue, Phys. Rev. Lett. **82**, 197 (1999).
[23] J. Martin, F. Cichos, and C. von Borczyskowski, Sol. Energy **108**, 347 (2004).
[24] X. Brokmann, J.-P. Hermier, G. Messin, P. Desbiolles, J.-P. Bouchaud, and M. Dahan, Phys. Rev. Lett. **90**, 120601 (2003).
[25] A. L. Efros and M. Rosen, Phys. Rev. Lett. **78**, 1110 (1997).
[26] K. T. Shimizu, W. K. Woo, B. R. Fisher, H. J. Eisler, and M. G. Bawendi, Phys. Rev. Lett. **89**, 117401 (2002).
[27] J. D. Casperson, L. D. Bell, and H. A. Atwater, J. Appl. Phys. **92**, 261 (2002).
[28] L. Bergmann and C. Schaefer, *Lehrbuch der Experimentalphysik: Festkörper* (de Gruyter, Berlin, 1992).
[29] J. Bardeen, Phys. Rev. Lett. **6**, 57 (1960).
[30] B. Brar, G. D. Wilk, and A. C. Seabaugh, Appl. Phys. Lett. **69**, 2728 (1996).
[31] W. Feller, *An Introduction to Probability Theory and Its Applications*, 3rd ed. (Wiley, New York, 1970).
[32] Y. Jung, E. Barkai, and R. J. Silbey, J. Chem. Phys. **117**, 10980 (2002).